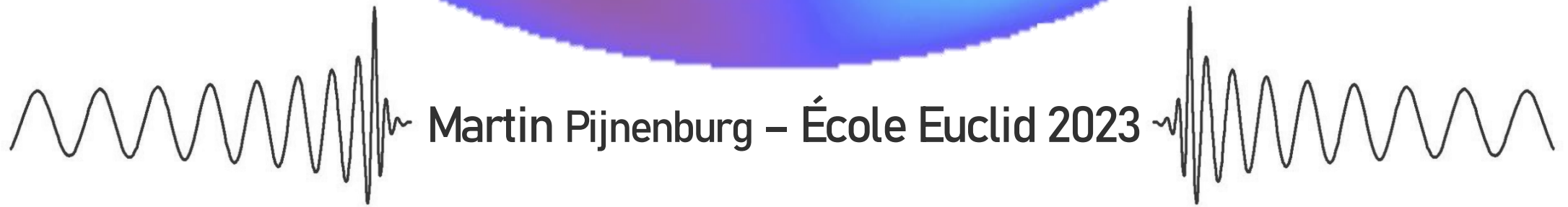


Gravitational wave events & the cosmic dipole tension



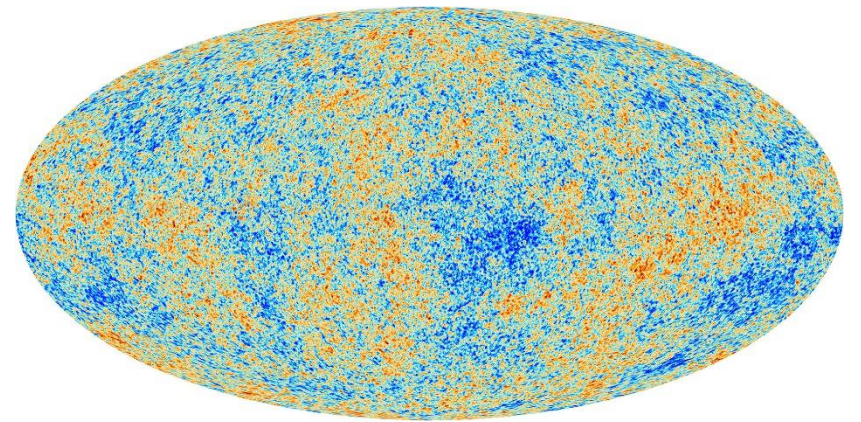
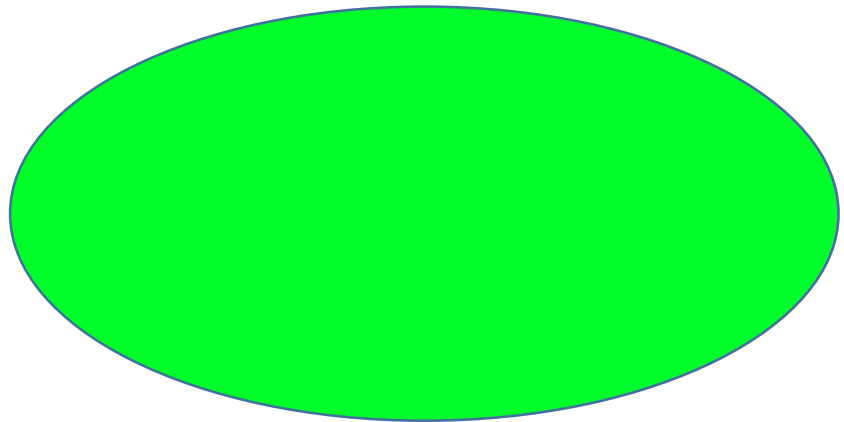
Martin Pijenburg – École Euclid 2023

The cosmological principle

« On large scales, the Universe is homogeneous and isotropic »

→ A pillar of cosmological theories (*FRWL*, etc.)

One illustration : CMB Temperature maps ...



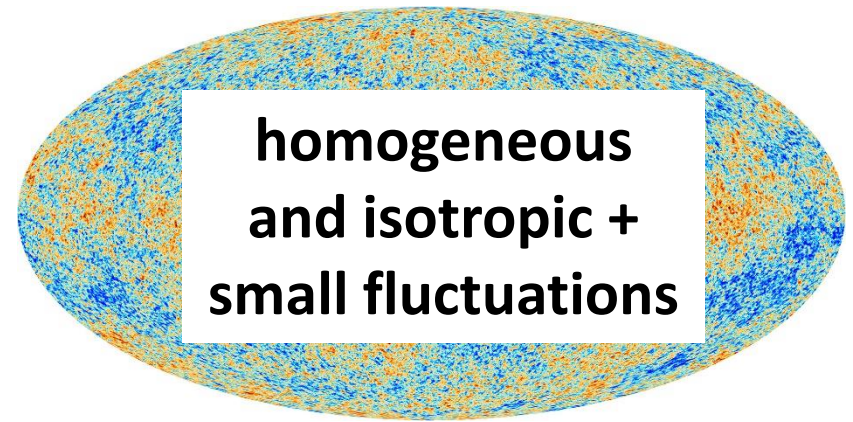
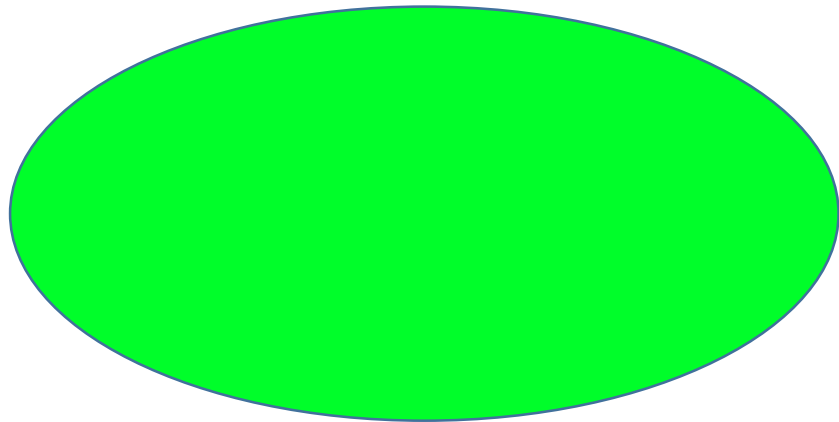
Credit : ESA and the Planck Collaboration

The cosmological principle

« On large scales, the Universe is homogeneous and isotropic »

→ A pillar of cosmological theories (*FRWL*, etc.)

One illustration : CMB Temperature maps ...

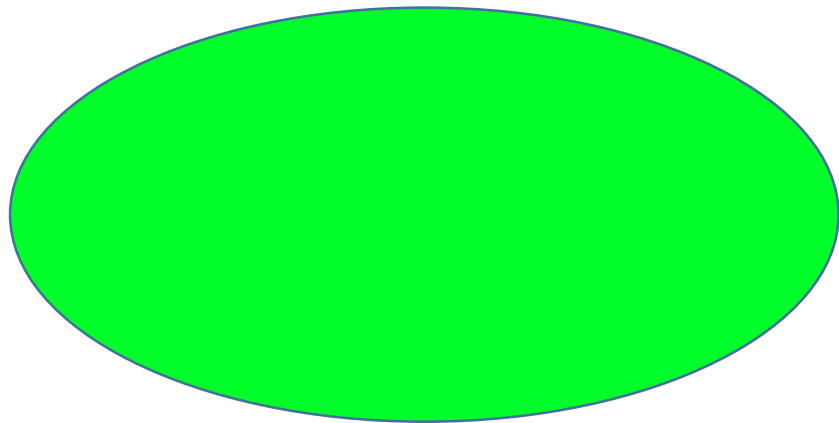


The cosmological principle

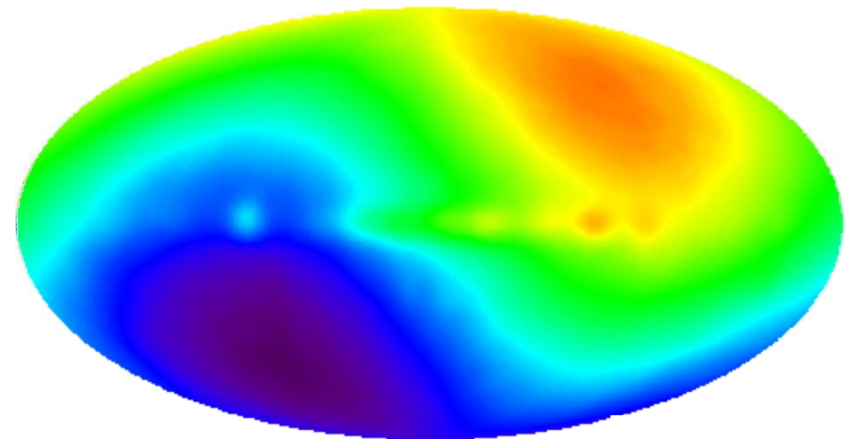
« On large scales, the Universe is homogeneous and isotropic »

→ A pillar of cosmological theories (*FRWL*, etc.)

One illustration : CMB Temperature maps ...



ACTUALLY



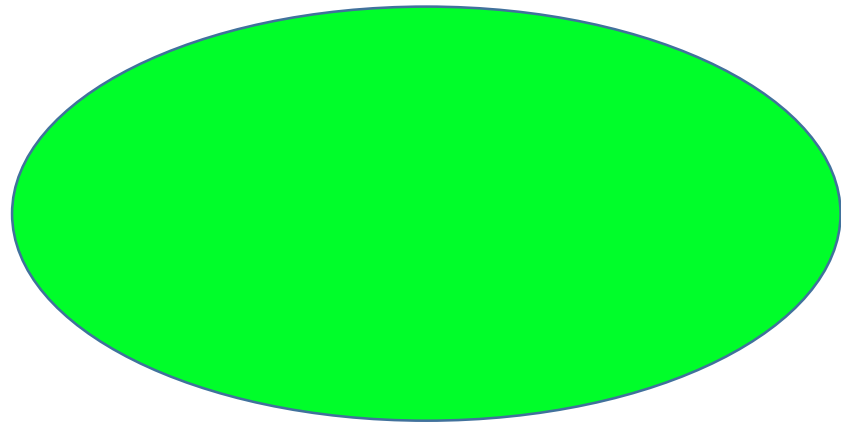
Credit : NASA / COBE Science Team

The cosmological principle

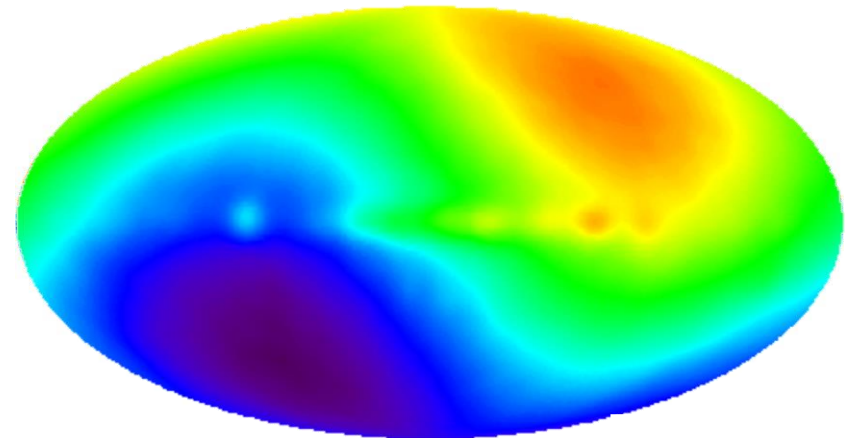
« On large scales, the Universe is homogeneous and isotropic »

→ A pillar of cosmological theories (*FRWL*, etc.)

One illustration : CMB Temperature maps ...



ACTUALLY



100 times stronger than
primordial perturbations

Credit : NASA / COBE Science Team

The cosmological principle

CMB has a dipole : Doppler effect interpretation

→ gives measure of our speed (direction & velocity) wrt CMB

Modulation factor $1 + z_{Doppler} = 1 - \hat{n} \cdot \mathbf{v}_0/c$

Planck found : $v_0/c \sim 1,2 \cdot 10^{-3}$

The cosmological principle

Interpretation:

- ★ Our local frame moving towards what looks like a “CMB rest frame”
- ★ This motion leads to a kinematic dipole observation
- ★ Can we say something similar with matter, in the late Universe ?

Kinematic dipole in matter maps: aberration

$$d\Omega = d\bar{\Omega} (1 - 2\hat{n} \cdot \mathbf{v}_0/c)$$

observed

at rest

Kinematic dipole in matter maps: aberration

$$d\Omega = d\bar{\Omega} (1 - 2\hat{\mathbf{n}} \cdot \mathbf{v}_0/c) \implies \frac{dN_{\text{events}}}{d\Omega} = \frac{dN_{\text{events}}}{d\bar{\Omega}} (1 + 2\hat{\mathbf{n}} \cdot \mathbf{v}_0/c)$$

observed at rest

→ universal to any distribution of events !

Kinematic dipole in matter maps: aberration

$$d\Omega = d\bar{\Omega} (1 - 2\hat{n} \cdot \mathbf{v}_0/c) \implies \frac{dN_{\text{events}}}{d\Omega} = \frac{dN_{\text{events}}}{d\bar{\Omega}} (1 + 2\hat{n} \cdot \mathbf{v}_0/c)$$

observed at rest

→ universal to any distribution of events !

★ Aberration: not the only source of kinematic dipole number counts
(population and selection effects can create dipoles, but object dependent)

Kinematic dipole in matter maps: chosen pieces in the literature

People looked at kinematic dipoles in :

★ quasars and radio sources at redshifts $0 \leq z \lesssim 3$.

(Colin et al. 2017; Bengaly et al. 2018; Secrest et al. 2021; Siewert et al. 2021; Secrest et al. 2022)

→ Direction ok with CMB but amplitude of velocity differs **up to 5.1σ**
i.e. up to factor 5 larger (*Secrest et al. 2022*)

★ :

.

Kinematic dipole in matter maps: chosen pieces in the literature

People looked at kinematic dipoles in :

★ quasars and radio sources at redshifts $0 \leq z \lesssim 3$.

(*Colin et al. 2017; Bengaly et al. 2018; Secrest et al. 2021; Siewert et al. 2021; Secrest et al. 2022*)

→ Direction ok with CMB but amplitude of velocity differs **up to 5.1σ**
i.e. up to factor 5 larger (*Secrest et al. 2022*)

★ Pantheon+ sample : *Sorrenti et al. 2022* find tension wrt CMB in velocity amplitude but also dipole direction

Gravitational waves :

What about using maps of detected GWs events ?

Yes, but...

Any non-perfect detector induces a **selection bias on the dipole** maps
(e.g. *Mastrogiovanni et al. 2023*)

→ Important to model it to get accurate results

The kinematic dipole in GW events

Taking the cumulative detections all along the line of sight:

$$\frac{dN_{\text{det}}}{d\Omega}(\hat{\mathbf{n}}) = \frac{d\bar{N}_{\text{det}}}{d\Omega} + \hat{\mathbf{n}} \cdot \frac{\mathbf{v}_0}{c} \left[2 + s \left(\frac{1}{3} + \mathcal{A} \right) \right] \frac{d\bar{N}_{\text{det}}}{d\Omega}$$

with s , \mathcal{A} functions encoding selection bias effects.

The kinematic dipole in GW events

Taking the cumulative detections all along the line of sight:

$$\frac{dN_{\text{det}}}{d\Omega}(\hat{\mathbf{n}}) = \frac{d\bar{N}_{\text{det}}}{d\Omega} + \hat{\mathbf{n}} \cdot \frac{\mathbf{v}_0}{c} \left[2 + s \left(\frac{1}{3} + \mathcal{A} \right) \right] \frac{d\bar{N}_{\text{det}}}{d\Omega}$$

with s, \mathcal{A} functions encoding selection bias effects.

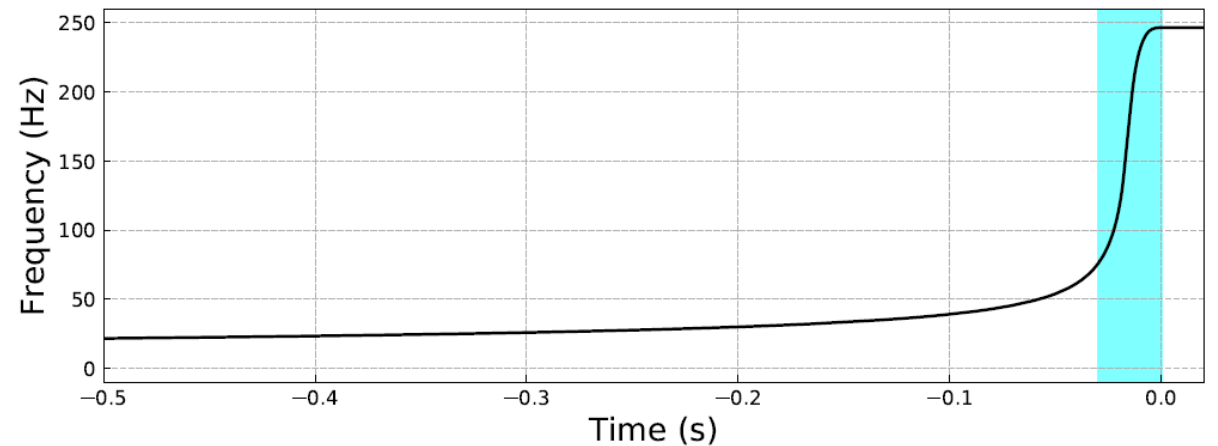
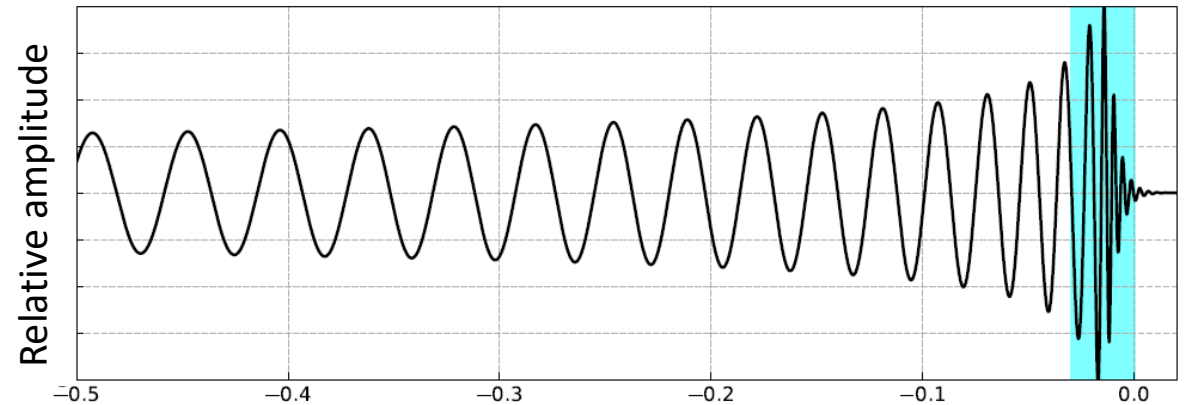
Once they are modelled, measure $\frac{dN_{\text{det}}}{d\Omega}(\hat{\mathbf{n}}), \frac{d\bar{N}_{\text{det}}}{d\Omega}$

→ extract \mathbf{v}_0 !

Gravitational waves (GW) signals

From the first phase of emission,
we observe the wave

- ★ Amplitude
- ★ Frequency
- ★ Frequency variation



Gravitational waves (GW) signals

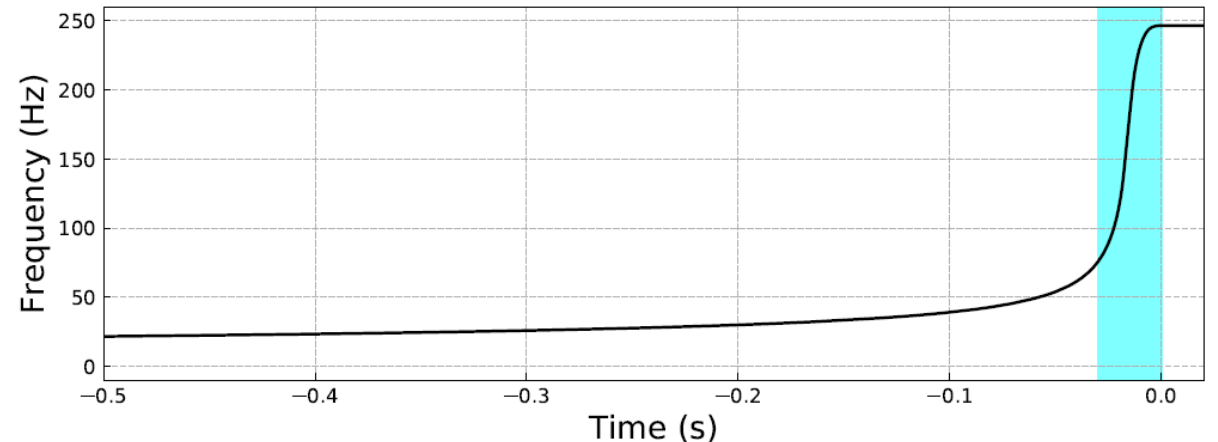
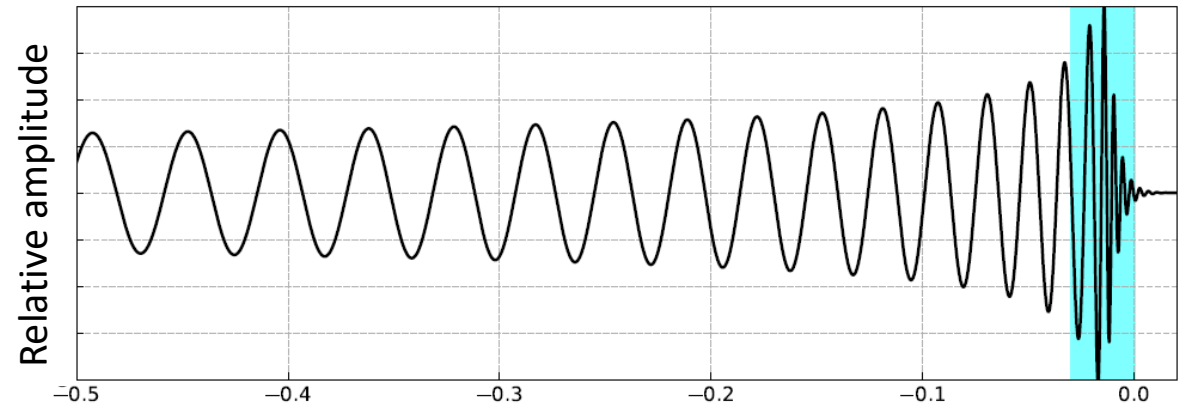
From the first phase of emission,
we observe the wave

- ★ Amplitude
- ★ Frequency
- ★ Frequency variation

From which we extract:

$$d_L = d_c (1 + z)$$

$$\mathcal{M}_z = \frac{(m_1 m_2)^{3/5}}{(m_1 + m_2)^{1/5}} (1 + z)$$



GWs : multiple estimators !

So far, only discussed maps of number counts of events.

★ Can also use maps of the distribution of detected \mathcal{M}_z & d_L

GWs : multiple estimators !

So far, only discussed maps of number counts of events.

- ★ Can also use maps of the distribution of detected \mathcal{M}_z & d_L
- ★ End up with 6 (correlated) estimators of the kinematic dipole: counts, \mathcal{M}_z & d_L maps, for both BBH and BNS

GWs : multiple estimators !

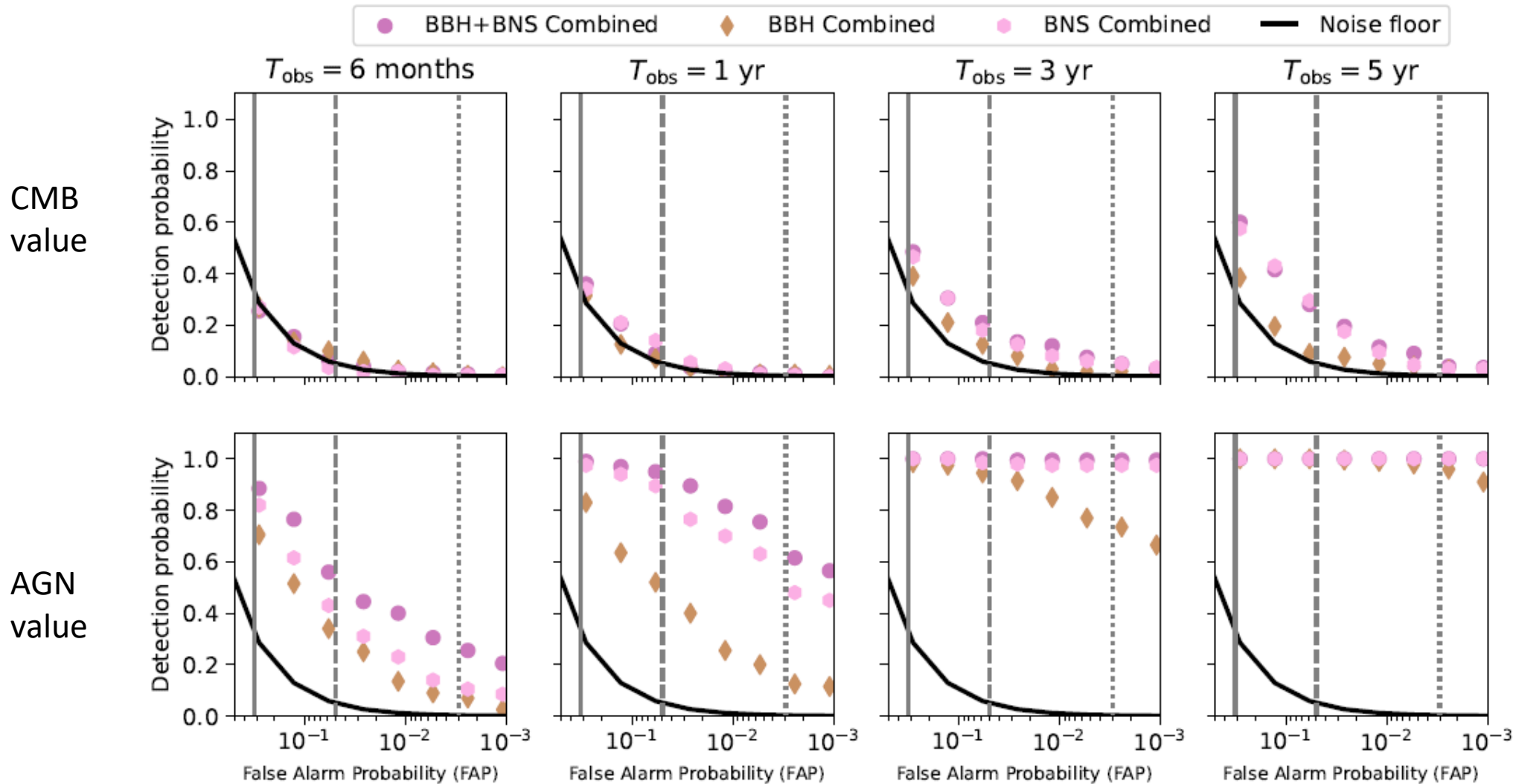
So far, only discussed maps of number counts of events.

- ★ Can also use maps of the distribution of detected \mathcal{M}_z & d_L
- ★ End up with 6 (correlated) estimators of the kinematic dipole: counts, \mathcal{M}_z & d_L maps, for both BBH and BNS
- ★ Combine them !

Next generation GW detectors (ET + CE)

- ★ Missions expecting to run in $O(10)$ years, reaching redshifts 50-100, detection of $\sim 10^5$ BBH and $\sim 10^5$ BNS events per year.
- ★ Negligible selection bias for BBH : over 99.9% of BBH events detected up to $z = 20$

Results for next generation GW detectors (ET + CE)



*Taken from
Grimm, MP,
et al., in prep.*

Fisher forecasts for next generation GW detectors (ET + CE)

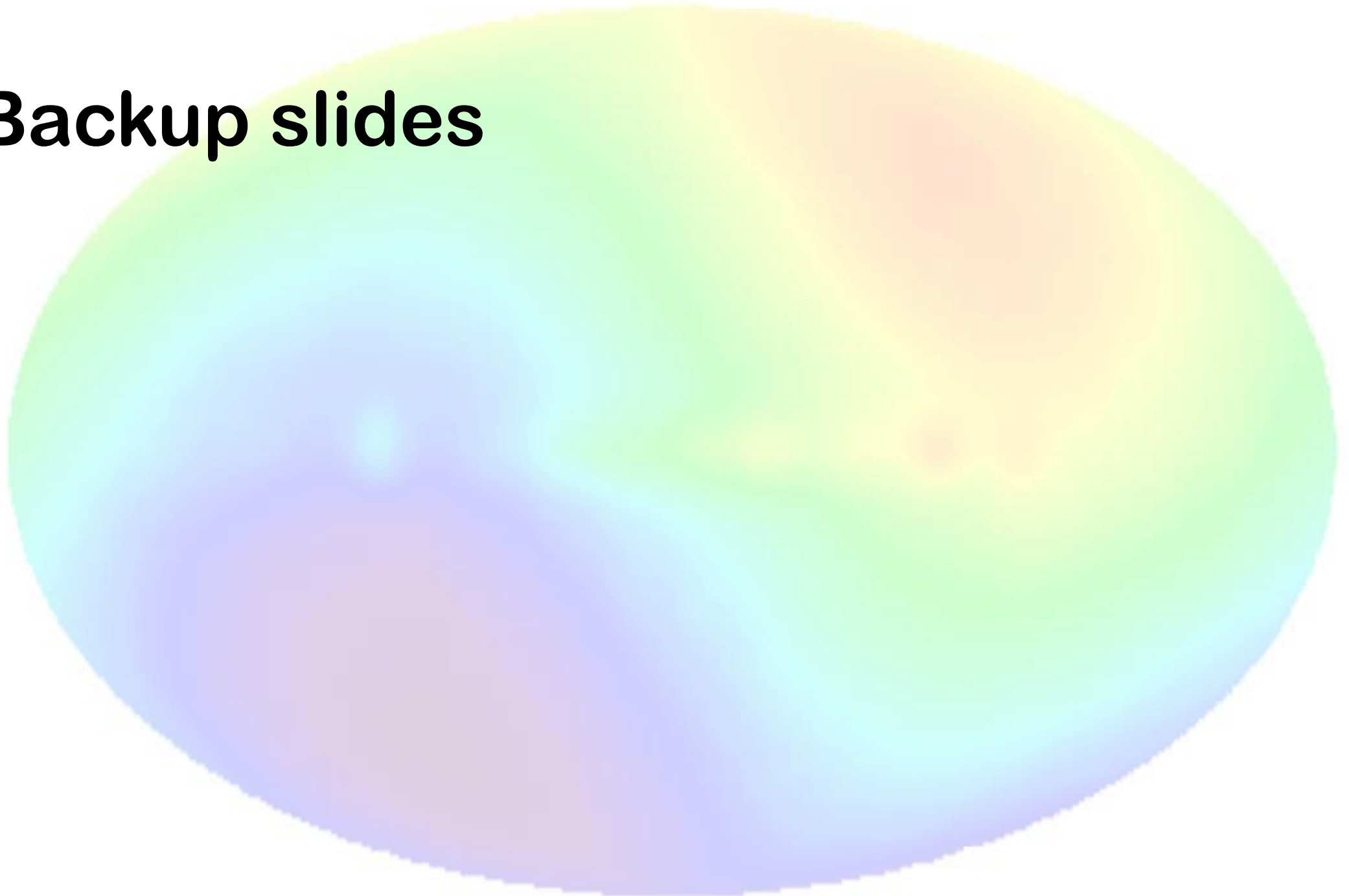
- ★ If the dipole in GWs maps is that of AGN, it will be detected at $\sim 2\sigma$ within 1 year of observation time
- ★ If the dipole is that of CMB, need 10 years for $\sim 1\sigma$ detection
- ★ Assuming their selection bias is controlled, BNS provide better constrains than BBH

Results for next generation GW detectors (ET + CE)

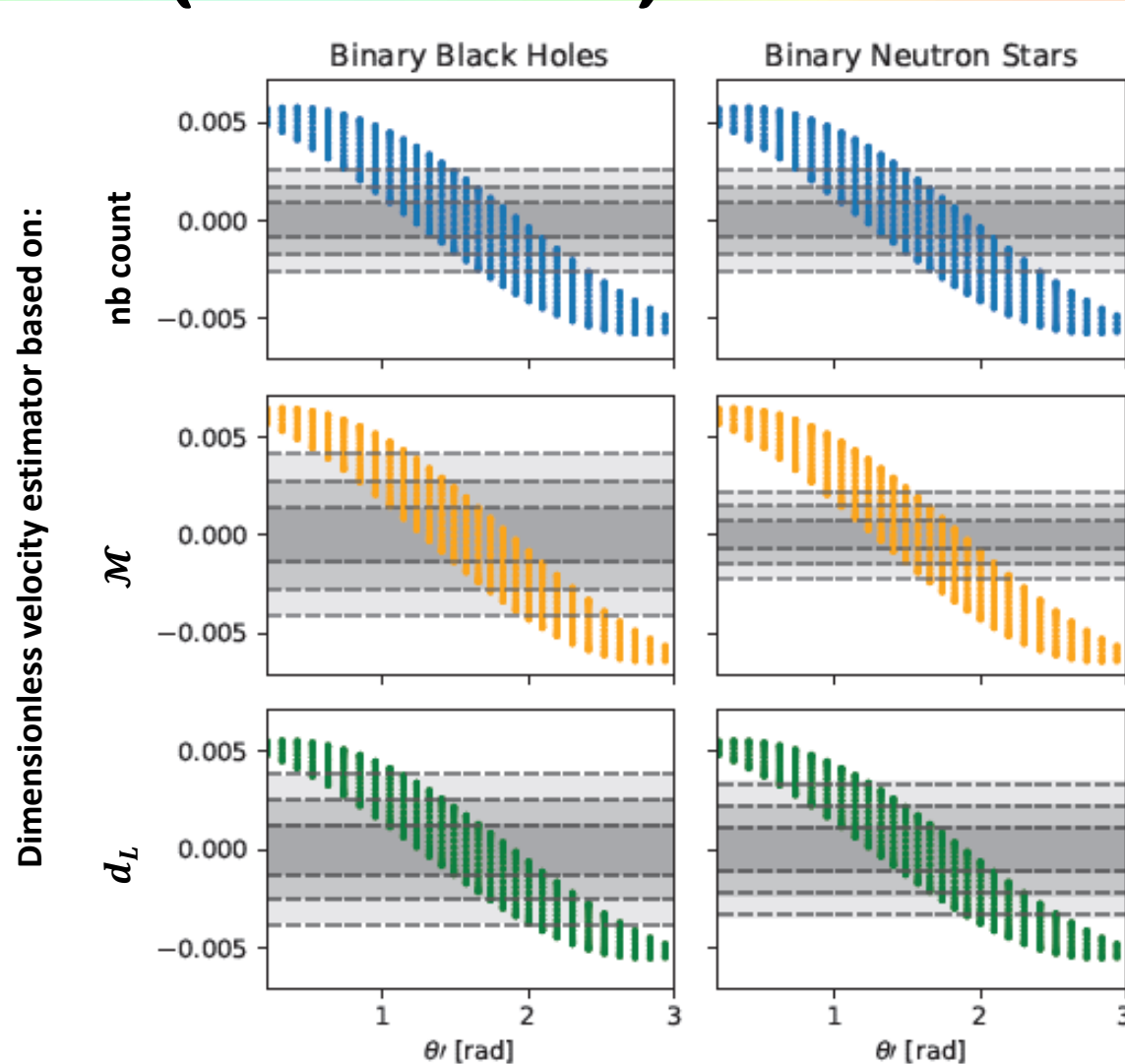
BNS : selection bias could account for $O(10\%)$ of the kinematic dipole

→ Selection bias cannot resolve a factor 5 tension in the value of the velocity

Backup slides



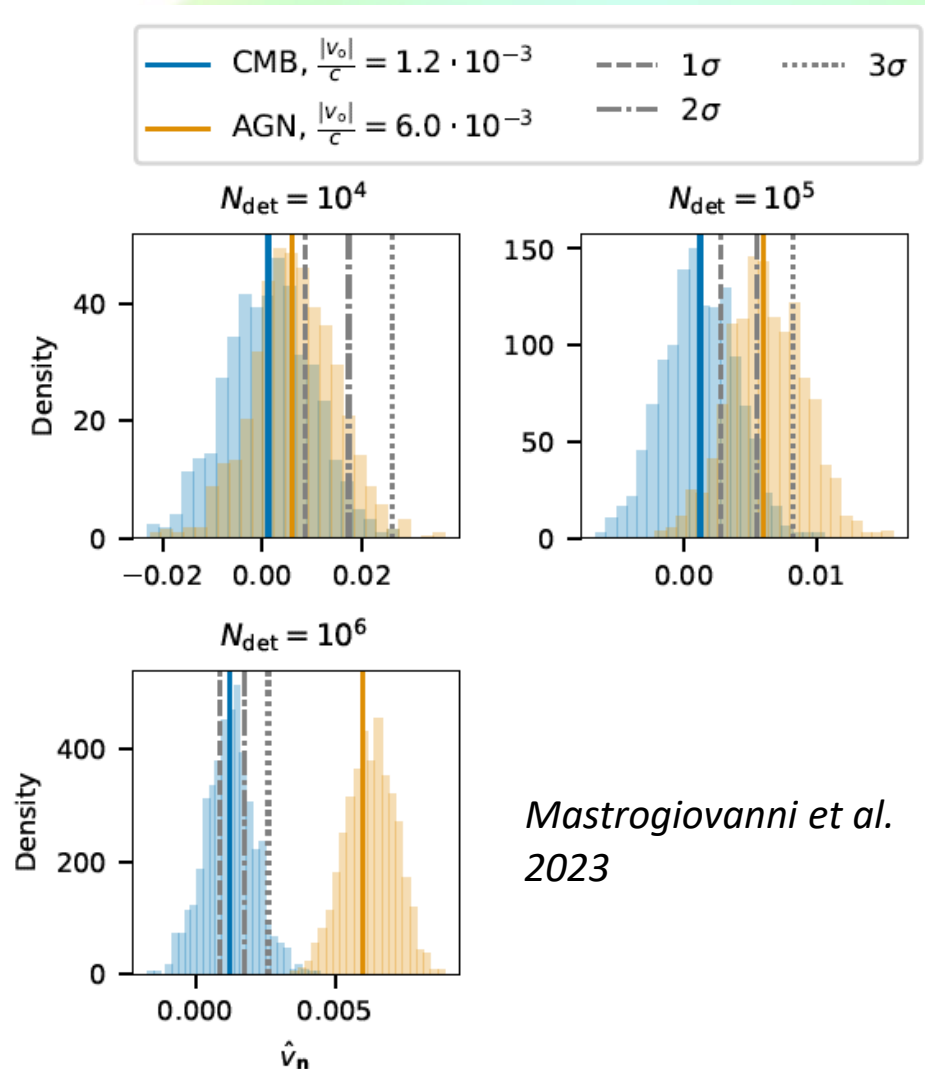
Results for next generation GW detectors (ET + CE)



Plot: 10 years
with
AGN dipole

*Taken from
Grimm, MP,
et al., in prep.*

Results for next generation GW detectors (ET + CE)



Mastrogiovanni et al.
2023

Figure 5. Distribution of the estimator \hat{v}_n evaluated in the injected velocity direction $\mathbf{n} = \hat{\mathbf{v}}_o$ with 10^4 , 10^5 , 10^6 and 10^7 BBH detections. The histograms are obtained by simulating 1000 populations of BBHs. The vertical dashed lines indicate the fiducial values of the GW dipole in the CMB case (blue) and the AGN case (orange). The dashed and dotted gray lines indicate the 1 , 2 , 3σ contribution from Poisson noise, generated using Eq. (27).

Results for next generation GW detectors (ET + CE)

Table 2. Error, $\sigma_{v_0/c}$, obtained from: the individual estimators (first 6 columns), combining the three BBH estimators, the three BNS estimators, all estimators, or using the top 3 combination of mass and number count estimator for BNSs and number count estimator for BBHs. In the top three rows, we consider a dipole consistent with the CMB one, while in the bottom three rows we consider a dipole consistent with the AGN one.

		\hat{v}_N^{BBH}	$\hat{v}_{d_L}^{\text{BBH}}$	\hat{v}_M^{BBH}	\hat{v}_N^{BNS}	$\hat{v}_{d_L}^{\text{BNS}}$	\hat{v}_M^{BNS}	BBH	BNS	All	Top 3
CMB	$N_{\text{tot}} = 10^5$	223%	327%	356%	206%	305%	194%	178%	139%	110%	119%
	$N_{\text{tot}} = 10^6$	70%	103%	113%	65%	96%	61%	56%	44%	35%	38%
	$N_{\text{tot}} = 10^7$	22%	33%	36%	21%	30%	19%	18%	14%	11%	12%
AGN	$N_{\text{tot}} = 10^5$	46%	67%	73%	42%	63%	40%	36%	29%	23%	24%
	$N_{\text{tot}} = 10^6$	14%	21%	23%	13%	20%	13%	12%	9%	7%	8%
	$N_{\text{tot}} = 10^7$	5%	7%	7%	4%	6%	4%	4%	3%	2%	2%

*Taken from
Grimm, MP,
et al., in prep.*

Results for BNS selection bias

$$\alpha = \frac{\text{expected dipole amplitude}}{\text{expected dipole amplitude from aberration}}$$

	α_N	α_{d_L}	α_M
BNS	1.08	0.94	0.98

*Taken from
Grimm, MP,
et al., in prep.*

Results for next generation GW detectors (ET + CE)

Table 3. Fisher bound on the error $\sigma_{v_0/c}$, obtained from the combination of the six estimators assuming different uncertainties on the α 's for the BNSs. In the top three rows, we consider a dipole consistent with the CMB one, while in the bottom three rows we consider a dipole consistent with the AGN one.

		10%	20%	50%
CMB	$N_{\text{tot}} = 10^5$	110%	110%	112%
	$N_{\text{tot}} = 10^6$	35%	36%	40%
	$N_{\text{tot}} = 10^7$	12%	13%	16%
AGN	$N_{\text{tot}} = 10^5$	23%	24%	28%
	$N_{\text{tot}} = 10^6$	8%	9%	11%
	$N_{\text{tot}} = 10^7$	3%	3%	4%

*Taken from
Grimm, MP,
et al., in prep.*

Gravitational waves : selection effects

What about using maps of detected GWs events ?

Yes, but... maps of GWs events can also be affected by another kinematic dipole that is **on top of aberration** :

simplified view:

we call «detected» only the events with signal above a certain

threshold

Gravitational waves : selection effects

What about using maps of detected GWs events ?

Yes, but... maps of GWs events can also be affected by another kinematic dipole that is **on top of aberration** :

Very simplified view:

★ let's call «detected» only the events with signal above a certain threshold

Gravitational waves : selection effects

→ Only the signal amplitude decides if an event is detected or not

$$d_L = d_c (1 + z)$$

But recall, signal amplitude contains

$$\mathcal{M}_z = \frac{(m_1 m_2)^{3/5}}{(m_1 + m_2)^{1/5}} (1 + z)$$

→ Those are z dependent and thus affected by Doppler shift

→ A given signal can be shifted above or below detection threshold,
creating dipole

Gravitational waves : selection effects

In practice, modelling this requires:

★ Specifying the noise sensitivity curves of the detector(s)

★ Estimating the intrinsic astrophysical distribution of binaries (in mass and distance)... to evaluate how many detections will be missed

★ This is poorly constrained for BNS

Gravitational waves : selection effects

In practice, modelling this requires:

- ★ Specifying the noise sensitivity curves of the detector(s)
- ★ Estimating the intrinsic astrophysical distribution of binaries (in masses and distance)... to evaluate how many detections will be missed

→ Last point is poorly constrained for BNS

Astrophysical population

We use the POWER LAW+PEAK model from [Abbott et al. \(2021b\)](#) to describe the source frame distribution of BBHs masses. This model is composed by two statistical distributions: a truncated power law distribution

$$\mathcal{P}(x|x_{\min}, x_{\max}, \alpha) \propto \begin{cases} x^{-\alpha} & (x_{\min} \leq x \leq x_{\max}) \\ 0 & \text{Otherwise.} \end{cases} \quad (\text{A1})$$

and Gaussian distribution with mean μ and standard deviation σ .

$$\mathcal{G}(x|\mu, \sigma) = \frac{1}{\sigma\sqrt{2\pi}} \exp\left[-\frac{(x-\mu)^2}{2\sigma^2}\right]. \quad (\text{A2})$$

The distribution of the source frame masses m_1, m_2 is factorized as

$$\pi(m_1, m_2|\Phi_m) = \pi(m_1|\Phi_m)\pi(m_2|m_1, \Phi_m), \quad (\text{A3})$$

where $\pi(m_1|\Phi_m)$ is the POWER LAW+PEAK model and $\pi(m_2|m_1, \Phi_m)$ is a truncated power law distribution. The secondary mass is conditioned to the constraint $m_2 < m_1$, i.e.

$$\pi(m_2|m_1, m_{\min}, \alpha) = \mathcal{P}(m_2|m_{\min}, m_1, \beta). \quad (\text{A4})$$

The POWER LAW+PEAK distribution is

$$\pi(m_1|m_{\min}, m_{\max}, \alpha, \lambda_g, \mu_g, \sigma_g) = (1 - \lambda_g)\mathcal{P}(m_1|m_{\min}, m_{\max}, -\alpha) + \lambda_g\mathcal{G}(m_1|\mu_g, \sigma_g) \quad (\text{A5})$$

where the power law part has slope $-\alpha$ between m_{\min} and m_{\max} , while the gaussian component has mean μ_g and standard deviation σ_g and accounts λ_g total fraction of the distribution. We also apply an additional smoothing at the lower edge of the distribution

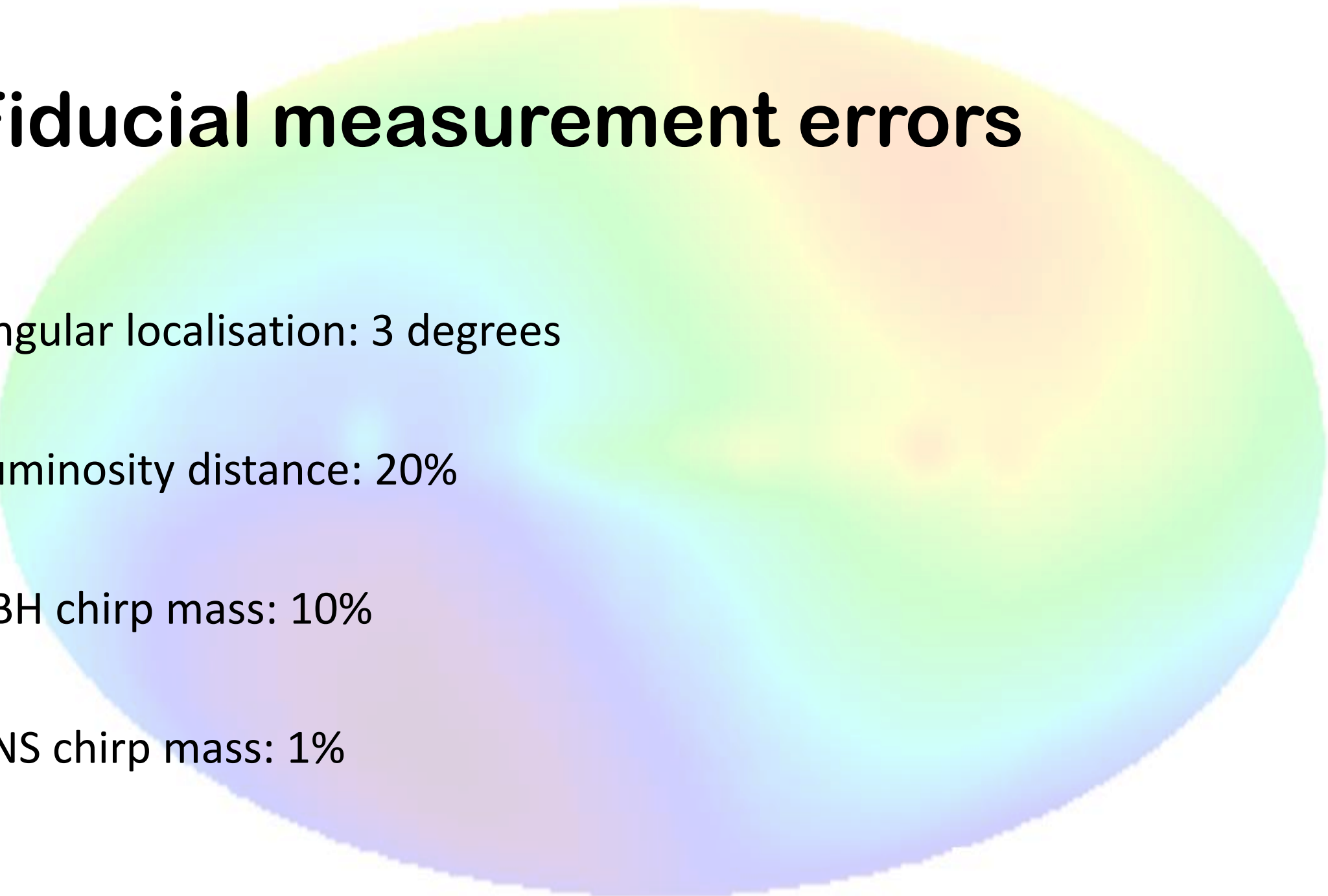
$$\pi(m_1, m_2|\Phi_m) = [\pi(m_1|\Phi_m)S(m_1|\delta_m, m_{\min})] \times [\pi(m_2|m_1, \Phi_m)S(m_2|\delta_m, m_{\min})] \quad (\text{A6})$$

where S is a sigmoid-like window function as described in [Abbott et al. \(2021b\)](#).

The parameters used for the simulation are $\alpha = 3.4, \beta = 1.1, m_{\max} = 87M_{\odot}, m_{\min} = 5.1M_{\odot}, \delta_m = 4.8M_{\odot}, \sigma_g = 3.6M_{\odot}, \mu_g = 34M_{\odot}, \lambda_g = 0.03$.

BNS : in mass range [1, 2.5] Msun, power law without peak

Fiducial measurement errors



Angular localisation: 3 degrees

Luminosity distance: 20%

BBH chirp mass: 10%

BNS chirp mass: 1%

Estimator correlations

Taken from
Grimm, MP,
et al., in prep.

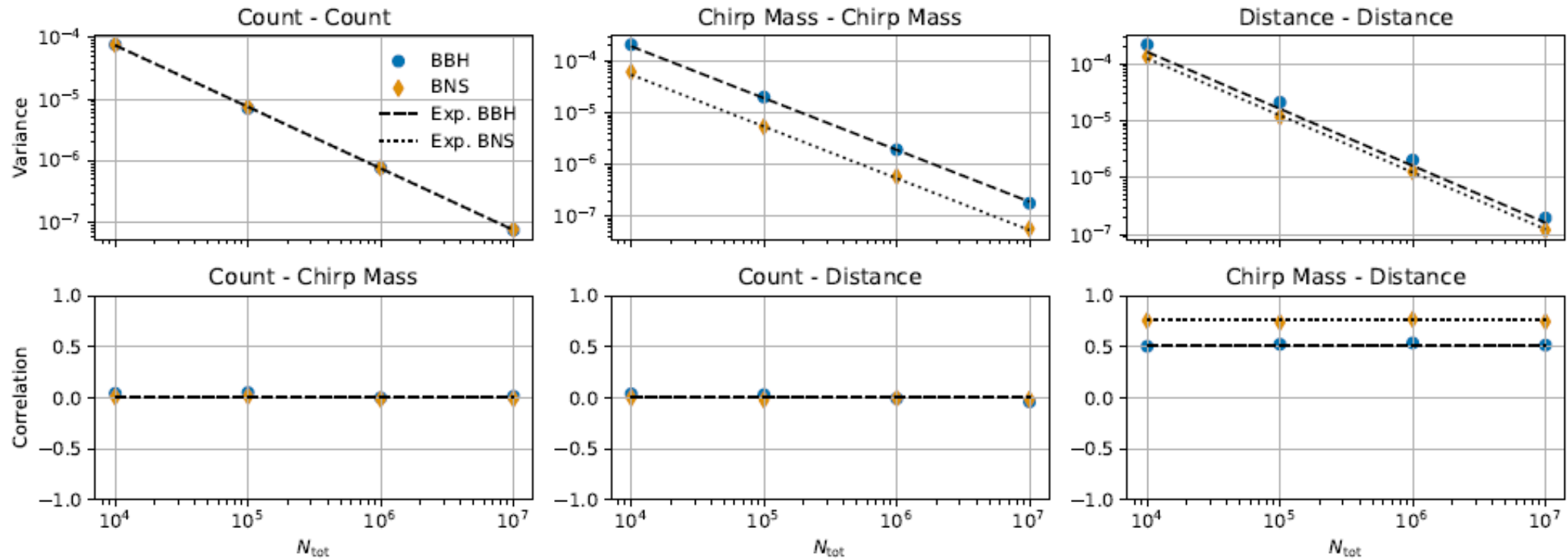


Figure 4. The plots report the variance (first row) and correlation (second row) of the number count, mass, and distance dipole estimators as a function of the number of detections N_{tot} . The variances and correlations are obtained by reshuffling 2'000 times isotropically a population of GW sources. The blue circles indicate the values obtained for the BBH population while the orange diamonds the values for the BNS population. The black lines (dashed for BBHs and dotted for BNSs) indicate the theoretical variance calculated in Sec. 3. The simulated correlations *number count - chirp mass* and *number count - luminosity distance* differ from zero by a few percent (due to the limited number of sky shufflings).

Number count estimator

$$v_{N-\mathbf{n}'} \equiv \frac{3}{2} \int \frac{d\Omega}{4\pi} (\mathbf{n} \cdot \mathbf{n}') \mathcal{D}N(\mathbf{n}) \simeq \alpha_N \frac{v_0}{c} \cos \theta' ,$$

$$\hat{v}_{N-\mathbf{n}'} = \frac{3}{2N_{\text{tot}}} \sum_{i=1}^{N_{\text{sky}}} N_{\text{det}}^i (\mathbf{n}_i \cdot \mathbf{n}') .$$

E.g. pixel size of 53 deg².

Einstein Telescope, Cosmic Explorer

Einstein Telescope (Europe):

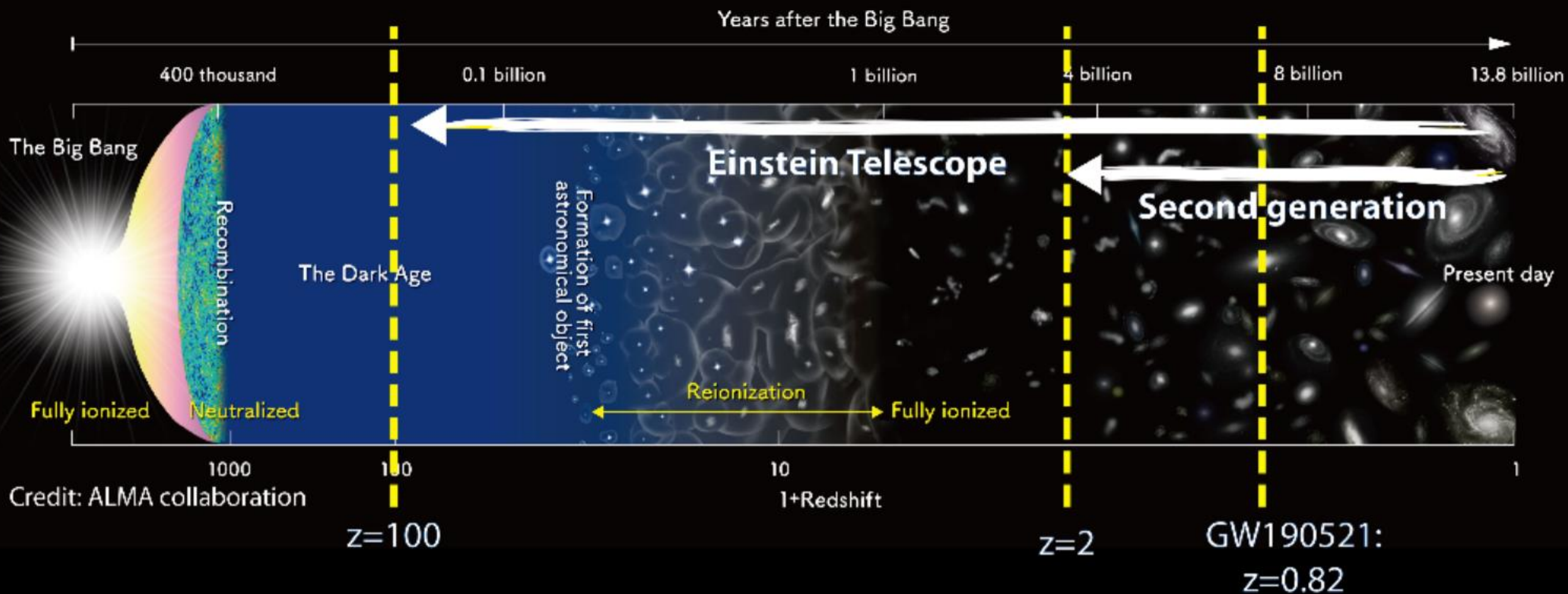
- ★ underground interferometers
- ★ arms 10km long (LIGO: 4km)

Cosmic Explorer (USA):

- ★ two ground based interferometers
- ★ arms 40km & 20km long

Einstein Telescope, Cosmic Explorer

Detection horizon for black-hole binaries



Gravitational wave signal parameters

For CBC: $15+2+2$ parameters

- intrinsic: 2 masses, $2*3$ spin vectors
- distance: 1
- time of coalescence: 1
- direction to the observer: 2 angles
- sky position in observer's frame: 2 angles
- polarization angle: 1 angle
- +eccentricity, periastron: 2
- +tidal deformabilities BNS: 2

Gravitational wave signal

c.f. Maggiore, *Gravitational Waves*, Oxford Univ. Press, 2008

$$ds^2 = -c^2 dt^2 + dz^2 + \{1 + h_+ \cos[\omega(t - z/c)]\} dx^2 \\ + \{1 - h_+ \cos[\omega(t - z/c)]\} dy^2 + 2h_\times \cos[\omega(t - z/c)] dx dy .$$

$$h_+(t_s) = h_c(t_s^{\text{ret}}) \frac{1 + \cos^2 \iota}{2} \cos \left[2\pi \int^{t_s^{\text{ret}}} dt'_s f_{\text{gw}}^{(s)}(t'_s) \right] ,$$

$$h_\times(t_s) = h_c(t_s^{\text{ret}}) \cos \iota \sin \left[2\pi \int^{t_s^{\text{ret}}} dt'_s f_{\text{gw}}^{(s)}(t'_s) \right] ,$$

$$h_c(t_{\text{obs}}^{\text{ret}}) = \frac{4}{d_L} \left(\frac{GM_c}{c^2} \right)^{5/3} \left(\frac{\pi f_{\text{gw}}^{(\text{obs})}(t_{\text{obs}}^{\text{ret}})}{c} \right)^{2/3}$$

Gravitational wave SNR

c.f. *L. Finn, D Chernoff, Phys. Rev. D, 1993*

$$\rho^2(r, \mathbf{n}, m, \mathcal{M}) = \frac{5}{96\pi^{4/3}} \frac{\Theta^2}{d_L^2(r, \mathbf{n})} (G\mathcal{M})^{5/3} \mathcal{F}\left(f_{\text{ISCO}}^z(m)\right), \quad (5)$$

where \mathcal{M} is the redshifted chirp mass as measured in the detector